DOI: 10.1002/ejic.201100315

Rational Design of Complex Borides – One-Electron-Step Evolution from Soft to Semi-Hard Itinerant Ferromagnets in the New Boride Series $Ti_2FeRu_{5-n}Rh_nB_2$ ($1 \leq n \leq 5$)

Boniface P. T. Fokwa,*[a] Heiko Lueken,[a] and Richard Dronskowski[a]

Dedicated to Professor John D. Corbett on the occasion of his 85th birthday

Keywords: Borides / Magnetic properties / Transition metals / Intermetallic phases / Valence electron count

The new $Ti_2FeRu_{5-n}Rh_nB_2$ series (n = 1–5) was synthesized by arc melting of stoichiometric amounts of the elements. These phases were characterized by X-ray diffraction methods as well as EDX measurements. All phases in the series are isostructural and crystallize with the $Ti_3Co_5B_2$ type structure (space group *P*4/*mbm*, no. 127). Magnetic susceptibility measurements reveal that all phases order ferromagnetically below Curie temperatures found between 220 and 390 K. Furthermore, a strong dependence of the coercive field as a function of VEC (valence electron count) is observed in the series: An evolution from soft (in the Rh-richer and VE-richer region) to semi-hard (in the Ru-richer and VE-poorer region) magnetic materials is found.

Introduction

Metal-rich borides, owing to their outstanding physical properties and applications, belong to one of the fascinating classes of materials, their magnetic phases being among the most exciting.[1–4] Ferro- and ferrimagnetic materials are usually divided into magnetically soft, semi-hard, and hard with regard to their applications.[5] Materials that contain magnetic centers exclusively represented by ferromagnetic transition metals often exhibit soft magnetic properties, reminiscent of the very soft ferromagnetic transition elements Fe, Co, Ni, and their alloys.[6] In this respect, the corresponding transition-metal-rich borides make no exception. For example, the technologically important iron borides are soft ferromagnets.[7]

Transition-metal-rich borides with the general formula $M_2M'T_5B_2$ (M = Mg or Sc; M′ = Fe, Co, Ni; T = Ru, Rh, Ir) have gained great importance both theoretically and experimentally.[8–13] They crystallize as ordered quaternary substitutional variants of the $Ti_3Co_5B_2$ type structure (space group *P*4/*mbm*).[14] Among the hitherto known complex borides with the above-mentioned general formula, some representatives with M = Ti and Zr were successfully synthesized only recently.[15,16] On account of an extraordinary structural unit, namely well-separated chains of magnetic 3d atoms M′ (Fe, Co, Ni) with intrachain and interchain separations of about 3.0 and 6.5 Å, respectively (see Figure 1), these metallic borides are outstanding examples to study itinerant magnetism, that is, magnetic moments carried by delocalized conduction electrons. Usually, in order to modify the magnetic properties of such materials, the magnetically active element has been replaced by a congener. We, however, have followed a different strategy by studying experimentally and theoretically the magnetic properties of transition-metal-rich borides as a function of the valence electron count (VEC), while the magnetically active element remains the same for a given series of isotypic compounds. The first set of compounds which has enabled a truly chemical fine-tuning of the magnetic properties was $Sc_2FeRu_{5-n}Rh_nB_2$ (series **1**) where n = 0, 1, ..., 5 with respective VEC = 60, 61, ..., 65.[12] The phases of series **1** differ exclusively in the ratio of the magnetically "silent" metals Ru and Rh. Upon varying the VEC from 60 to 65, that is, with increasing Rh content, the stepwise change of long-range magnetic ordering from strong antiferromagnetism (VEC = 60) to strong ferromagnetism (VEC = 65) was observed together with an increase in the magnetic saturation moment in the ferromagnetic range.[13] According to the recorded hysteresis loops, the ferromagnetic members of series **1** can be classified as soft materials, confirming the trend observed so far for nearly all ferromagnetic metal-rich borides. In addition, the electronic and magnetic properties have been calculated by using density functional theory,[13] which reveals a correlation between the size of the magnetic saturation moment and the VEC, analogous

[a] Institut für Anorganische Chemie, RWTH Aachen University, 52056 Aachen, Germany
E-mail: boniface.fokwa@ac.rwth-aachen.de

Supporting information for this article is available on the WWW under http://dx.doi.org/10.1002/ejic.201100315.

to the measured data. The $Sc_2FeRu_{5-n}Rh_nB_2$ series is, until now, the only complete series of phases with the general formula $M_2M'T_{5-n}T'_nB_2$. In fact, three other series have been reported recently, $Zr_2Fe_{1-\delta}Ru_{5-x+\delta}Rh_xB_2$ ($\delta < 0.15$, x = 0, 1),[15] $Ti_2FeRu_{5-x}Ir_xB_2$ (x = 1–4), and $Zr_2Fe_{1-\delta}Ru_{5-x+\delta}Ir_xB_2$ ($\delta < 0.15$, x = 1–2);[16] however, none of them is a complete series. We have now achieved the synthesis of the second nearly complete series $Ti_2FeRu_{5-n}Rh_nB_2$ (series **2**), where n = 1, 2, ..., 5 corresponds to VEC = 63, 64, ..., 67. As in the $Ti_2FeRu_{5-x}Ir_xB_2$ series, the member with n = 0 (or x = 0) was not obtained. Nevertheless, series **2** offers another possibility to study not only the evolution of the magnetic properties as a function of the VEC but also the influence of the substitution of the magnetically "silent" titanium for the equally magnetically "silent" scandium.

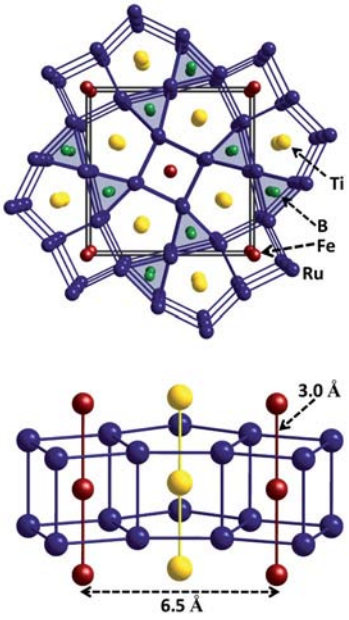

Figure 1. Perspective view of the crystal structure of the compound series $Ti_2FeRu_{5-n}Rh_nB_2$ along the [001] direction (top) and a part of the structure showing the intrachain (ca. 3.0 Å) and interchain (ca. 6.5 Å) Fe–Fe distances (bottom).

Results and Discussion

On the basis of X-ray powder data, the lattice parameters (a, c) of the five compounds of series **2** could be refined, and the $Ti_3Co_5B_2$ type structure was confirmed. Similar to the trend in lattice dimensions of the isoelectronic species of series **1** (n = 3, 4, 5[12]) and of the isotypic solid solutions $Sc_{1-x}Si_xIr_5B_2$[9] and $Ti_2FeRu_{5-x}Ir_xB_2$,[16b] a and c vary in opposite directions (see Supporting Information, Figure S1) when keeping the volume nearly constant at approximately 248 Å^3 (see Table 2). Single-crystal structure analyses of all members of series **2** confirmed the order of titanium, iron, and boron atoms on their respective positions as well as the order of rhodium in the case of $Ti_2FeRh_5B_2$. For the phases containing both ruthenium and rhodium, the ratios Ru/Rh were quantitatively determined by using energy dispersive X-ray analysis (EDX) on several crystals. These ratios confirmed the nominal ones and were imposed on the single-crystal structure refinements. Interatomic distances, especially those within and between the Fe–Fe chains (2.97 to 3.01 Å and 6.45 to 6.50 Å, respectively; see Figure 1, bottom) compare well with those observed in series **1** and in related ternary as well as quaternary transition metal borides consisting of at least three of the elements of series **2**.[17]

As mentioned in the Introduction already, upon varying the VEC in series **1** from 60 to 65, the stepwise change of long-range magnetic ordering from strong antiferromagnetism (VEC = 60) to strong ferromagnetism (VEC = 65) was observed together with an increase of the magnetic saturation moment in the ferromagnetic range.[12] The substitution of scandium in series **1** by titanium to produce series **2** leads to a shifting of the VEC range from VEC = 60–65 in the first to VEC = 63–67 in the second (the 62 VE phase was not achieved in series **2**). Therefore, both series overlap in the VEC range VEC = 63–65, which corresponds to the ferromagnetic range in series **1**. The analysis of the lattice parameters (see above) of both series suggests a similar behavior in their common VEC range; thus, because the magnetically active element (Fe) is the same in both series, a similar long-range magnetic ordering may be expected in series **2**. Indeed, thermomagnetic investigations (2–400 K) of the compounds of series **2** have revealed throughout the evolution of ferromagnetism in a wide temperature range and the transition to paramagnetism at higher temperatures as in series **1** (see Supporting Information, Table S1). Controlled by VEC, clear trends in the magnetic characteristics are evident in both the ferromagnetic and the paramagnetic range (see Table 1). Regarding the magnetically ordered state, the increase in VEC from 63 to 66 produces increasing ferromagnetic interactions, expressed by increasing atomic

Table 1. Magnetic values for series **2** ($Ti_2FeRu_{5-n}Rh_nB_2$).

n	VEC	Curie–Weiss range C /m^3 K mol^{-1}	μ [a] /μ_B	θ /K	T_{CW}[b] /K	T_C /K	Hysteresis loops μ_a[c] /μ_B	H_c[d] /kA m^{-1}
1	63	2.2×10^{-5}	3.7	+175	≥ 250	220	0.6	23.9
2	64	3.9×10^{-5}	5.0	+230	≥ 300	285	1.7	10.3
3	65	–	–	–	> 400[e]	390	2.2	1.6
4	66	–	–	–	> 400[e]	≥ 350	3.1	2.4
5	67	4.1×10^{-5}	5.1	+200	≥ 250	208	2.3	0.9

[a] μ: Magnetic moment, calculated from the Curie constant (C) of the Curie–Weiss straight line. [b] T_{CW}: Lowest temperature of the Curie–Weiss range. [c] μ_A: Atomic magnetic dipole moment ($\mu_a = M_m/N_A$, measured in Bohr magnetons[20]) at T = 5 K and B_0 = 4.5 T. [d] H_c: Coercivity obtained from the hysteresis loops at 5 K and $-4.5 \leq B_0 \leq 4.5$ T. [e] Curie–Weiss (CW) behavior expected.

magnetic dipole moments (μ_a) (recorded at 5 K and B_0 = 4.5 T, see Figure 2a and Figure S2 in the Supporting Information) from μ_a = 0.6 μ_B (VEC = 63) to μ_a = 3.1 μ_B (VEC = 66) and increasing Curie temperatures from T_C = 220 K (VEC = 63) to 390 K (VEC = 66). [Note that the T_C values of the samples with VEC = 63, 64, 66, and 67 were deduced from the intersection of a linear fit of the steepest part of the μ_a vs. T plots at a weak applied field B_0 = 0.1 T (see, for example, Figure 2a), while for VEC = 65 only the lower limit of T_C was estimated]. The final VEC step from 66 to 67 yields a distinct decrease in the magnetic values to μ_a = 2.3 μ_B and T_C = 208 K. This behavior is probably responsible for the upturn observed for the lattice parameters a and c at VEC = 67 (see Supporting Information, Figure S1). Obviously, the phase with VEC = 66 stands out from the others on account of a maximum in the ferromagnetic characteristics at this VEC. This finding is supported by first principles density functional studies, which have predicted a maximum value of the atomic saturation magnetization at VEC = 66 on the basis of the analysis of electronic DOS (density of states) curves of several intermetallic borides.[18]

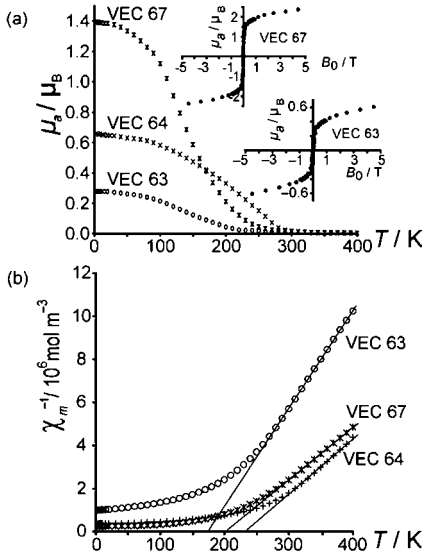

Figure 2. (a) μ_a vs. T [recorded at B_0 = 0.1 T], inset: hysteresis loops at 5 K for phases with VEC = 63 and 67. (b) χ_m^{-1} vs. T plots [recorded at B_0 = 4.5 T] for $Ti_2FeRu_4RhB_2$ (VEC 63), $Ti_2FeRu_3Rh_2B_2$ (VEC 64), and $Ti_2FeRh_5B_2$ (VEC 67); the solid lines are just guides for the eyes.

Referring to the paramagnetic behavior, a sufficient temperature interval, necessary for a reliable evaluation of the paramagnetic range, exists only for the phases with VEC = 63, 64, and 67. From a χ_m^{-1} vs. T plot, displayed in Figure 2b, Curie–Weiss behavior, $\chi_m = C/(T - \theta)$, is evident. The values obtained for the Curie constant C, the corresponding magnetic moment μ, and the Weiss constant θ are listed in Table 2. By comparing the magnetic characteristics of the paramagnetic and ferromagnetic regions, similar trends can be observed: a pronounced incremental step of C, θ, T_C, and μ_a upon increasing VEC from 63 to 64 [C = 2.2 to 3.9 (10^{-5} m^3 K mol^{-1}), θ = 175 to 230 K, T_C = 220 to 285 K, μ_a = 0.6 to 1.7 μ_B]. On account of the small paramagnetic region of the phases with VEC = 65 and 66, their paramagnetic characteristics are not available. So, the full trend within the paramagnetic regions of the series **2** members is not examinable, but the available magnetic data for VEC = 67 ($C = 4.1 \times 10^{-5}$ m^3 K mol^{-1}, θ = 200 K) are found in plausible ranges.

Special attention is finally devoted to the hysteresis measurements performed at 5 K and applied fields –4.5 T ≤ B_0 ≤ +4.5 T. Figure 3(a–e) is, however, restricted to the fundamental details of the hysteresis loops μ_a vs. B_0 for all phases (complete hysteresis loops are given in the Supporting Information, Figure S2). The essence of the μ_a vs. H diagram in Figure 3f is to classify the hardness of these ferromagnetic borides by the coercivity H_c (H_c < 1 kA m^{-1} stands for "soft" and H_c > 30 kA m^{-1} for "hard").[2,5] Inspecting Figure 3f and Table 2, the H_c values measured for series **2** increase with decreasing VEC. While for the sample with VEC = 67 the coercivity is 0.9 kA m^{-1} corresponding to a soft magnetic material, the H_c values grow dramatically to 10.3 kA m^{-1} at VEC = 64 and finally to 23.9 kA m^{-1} at VEC = 63, that is, within the "semi-hard" region. Therefore an evolution from soft to semi-hard ferromagnetic materials is obtained when VEC decreases from 67 to 63. This behavior was observed neither in series **1** nor in other transition metal borides reported so far,[12b] as all ferromagnetic phases were found to be magnetically soft. Therefore, the presence of titanium in a Ru-rich boride phase may be the

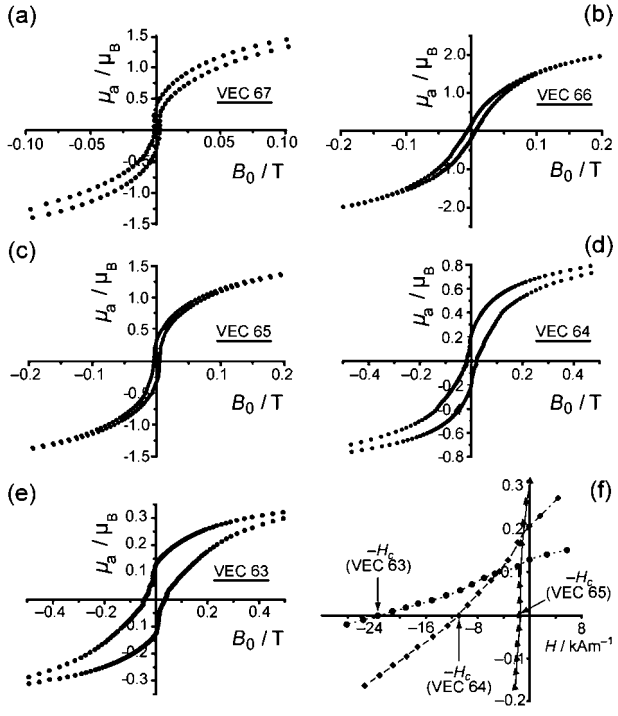

Figure 3. (a–e) Central parts of the hysteresis loops μ_a vs. H [recorded at 5 K and –4.5 ≤ B_0 ≤ 4.5 T] showing their enlargement with decreasing valence electron count (VEC) from 67 to 63. (f) Enlarged left parts of these hysteresis loops showing the increasing coercivity H_c with decreasing VEC.

driving force behind this exciting behavior. We are currently targeting more ferro- or ferrimagnetic ruthenium-rich boride phases containing titanium, in order to get more insight into this discovery.

Conclusions

We have shown that the substitution of the magnetically "silent" scandium in $Sc_2FeRu_{5-n}Rh_nB_2$ series by the equally "silent" titanium has led to the discovery of the new ferromagnetic $Ti_2FeRu_{5-n}Rh_nB_2$ series. In this series, the variation of the Ru/Rh ratio, that is, the decrease of VEC from 67 to 63, leads to the evolution from soft (Rh-rich phases) to semi-hard (Ru-rich phases) ferromagnetic materials. All phases have high Curie temperatures, which are all between 220 and 390 K.

Experimental Section

Synthesis: Polycrystalline samples and single crystals of the series $Ti_2FeRu_{5-n}Rh_nB_2$ (n = 1, 2, 3, 4, 5) were successfully synthesized by arc-melting the elements. For more details, see synthesis of series **1**.[12] According to powder X-ray diffractograms, all ruthenium-rich phases and $Ti_2FeRu_2Rh_3B_2$ are single-phase, but $Ti_2FeRuRh_4B_2$ and $Ti_2FeRh_5B_2$ are slightly contaminated by the Ti_2Rh_6B phase. As it is almost impossible to differentiate rhodium and ruthenium in the same compound by means of X-ray diffraction (they differ from each other by just one electron), the Ru/Rh ratio was very well characterized by energy dispersive X-ray analysis (EDX) with a high-resolution, low-energy SEM of the type LEO 1530 (Oberkochen, Germany) equipped with an EDX system of the type INCA (Oxford, England). EDX measurements on several selected crystals provided the same Fe/Ti ratio (1:2.07) for all compounds: The Ru/Rh ratios 4.03:1, 3.08:2, 2:3.10, and 1:4.05 (averaged experimental data; the standard deviation was about 0.03 in each case) were obtained for $Ti_2FeRu_4RhB_2$, $Ti_2FeRu_3Rh_2B_2$, $Ti_2FeRu_2Rh_3B_2$, and $Ti_2FeRuRh_4B_2$ respectively.

Structure Determination: The isotypic $Sc_2FeRu_{5-n}Rh_nB_2$ structures[12] were used as starting models for the structure refinements,[19] replacing Sc by Ti (Table 2). When these starting models are used, the refinements converge rapidly. It is worth mentioning that direct methods were also applied to solve the structures, and the same results were obtained. Replacing rhodium by ruthenium in the structure does not influence the refinements, as expected. Therefore the Ru/Rh ratios obtained from the EDX analyses were imposed to the structure models for the final proper refinements. Further details on the crystal structure investigations may be obtained from the Fachinformationszentrum Karlsruhe, 76344 Eggenstein-Leopoldshafen, Germany (Fax: +49-7247-808-666, E-mail: crysdata@fiz-karlsruhe.de) on quoting the depository numbers CSD-380367 (for $Ti_2FeRh_5B_2$), -380368 (for $Ti_2FeRu_2Rh_3B_2$), -380369 (for $Ti_2FeRu_3Rh_2B_2$), -380370 (for $Ti_2FeRu_4RhB_2$), and -380371 (for $Ti_2FeRuRh_4B_2$).

Magnetic Measurements: The magnetic measurements were carried out on polycrystalline samples (mainly selected crystals, weighed portions 9–15 mg) by using a SQUID magnetometer [MPMS-5S, Quantum Design, San Diego, USA; temperature range $4 \leq T \leq 400$ K, applied field up to 4.5 T]. The samples were prepared by manual selection of large crystals under an optical microscope. These were then coarsely ground and encapsulated in quartz tubes. Details of sample arrangement and measurement technique are described elsewhere.[20] Corrections for diamagnetic and conduction electron contributions were not applied, but demagnetization corrections were applied for all hysteresis loops.

Supporting Information (see footnote on the first page of this article): Additional magnetic and structural data.

Table 2. Crystallographic data for $Ti_2FeRu_4RhB_2$ (63 VE), $Ti_2FeRu_3Rh_2B_2$ (64 VE), $Ti_2FeRu_2Rh_3B_2$ (65 VE), $Ti_2FeRuRh_4B_2$ (66 VE), and $T_2FeRh_5B_2$ (67 VE).

Formula	$Ti_2FeRu_4RhB_2$	$Ti_2FeRu_3Rh_2B_2$	$Ti_2FeRu_2Rh_3B_2$	$Ti_2FeRuRh_4B_2$	$Ti_2FeRh_5B_2$
Formula weight	680.46	682.30	684.14	685.98	687.82
$F(000)$	602	604	606	608	610
Crystal size /mm^3	0.10 × 0.04 × 0.04	0.11 × 0.03 × 0.02	0.06 × 0.03 × 0.03	0.09 × 0.02 × 0.02	0.09 × 0.04 × 0.04
Diffractometer	Bruker APEX CCD, Mo-K_α, graphite monochromator				
h, k, l range	$-14 \leq h \leq 12$ $-14 \leq k \leq 13$ $-4 \leq l \leq 4$	$-14 \leq h \leq 14$ $-14 \leq k \leq 14$ $-4 \leq l \leq 4$	$-15 \leq h \leq 13$ $-12 \leq k \leq 14$ $-4 \leq l \leq 4$	$-14 \leq h \leq 14$ $-11 \leq k \leq 15$ $-4 \leq l \leq 4$	$-12 \leq h \leq 14$ $-14 \leq k \leq 14$ $-4 \leq l \leq 4$
θ-range /°	$3.15 \leq \theta \leq 36.13$	$3.15 \leq \theta \leq 36.10$	$3.14 \leq \theta \leq 35.83$	$4.97 \leq \theta \leq 35.67$	$3.17 \leq \theta \leq 35.60$
Collected reflections	4258	8394	4160	2576	4174
Independent reflections	353	355	352	347	351
Obs. reflections $I > 2\sigma(I)$	319	328	334	325	309
R_{int}; R_{sigma}	0.0309; 0.0177	0.0315; 0.0126	0.0226; 0.0140	0.0423; 0.0281	0.0473; 0.0256
Space group; Z	$P4/mbm$ (no. 127); 2				
Lattice parameters a /Å	9.1507(11)	9.1590(8)	9.1790(9)	9.1703(13)	9.0833(8)
c /Å	2.9682(6)	2.9586(5)	2.9526(5)	2.9521(7)	3.0127(5)
V /Å^3	248.54(7)	248.19(5)	248.77(5)	248.26(8)	248.57(5)
Calcd. density /g cm^{-3}	9.09	9.13	9.13	9.18	9.19
Abs. correction	Semi-empirical				
Abs. coefficient	20.74	21.05	21.28	21.61	21.86
T_{min}; T_{max}	0.239; 0.499	0.204; 0.678	0.361; 0.568	0.245; 0.673	0.244; 0.475
Refinement	SHELX-97, full-matrix against F^2				
Parameters/restraints	19/0	19/0	19/0	19/0	19/0
R_1; wR_2 (all I)	0.0328; 0.0612	0.0292; 0.0594	0.0312; 0.0665	0.0689; 0.1452	0.0521; 0.0965
GooF	1.23	1.13	1.21	1.62	1.14
Diff. peak/hole /e Å^{-3}	1.28 / –3.18	1.69 / –3.03	1.53 / –2.15	3.03 / –3.08	2.11 / –3.21

Acknowledgments

The authors thank Deutsche Forschungsgemeinschaft (DFG) for financial support, Klaus Kruse and Dr. Manfred Speldrich for measurement of the magnetic data, and Resi Zaunbrecher (IPC, RWTH Aachen) for the EDX analyses. B. P. T. Fokwa is grateful to the DFG for awarding him the Heisenberg fellowship.

[1] B. D. Cullity, C. D. Graham, *Introduction to Magnetic Materials*, 2nd ed., Wiley, New Jersey, **2009**.
[2] S. Chikazumi, *Physics of Ferromagnetism*, Clarendon, Oxford, **1997**.
[3] H. Lueken, *Magnetochemie*, Teubner, Stuttgart, **1999**.
[4] a) J. F. Herbst, *Rev. Mod. Phys.* **1991**, *63*, 819–898; b) The best hard magnetic materials (at room temperature) known to date are metal-rich borides with the general formula $Ln_2Fe_{14}B$ (Ln = lanthanoid element) having extremely high coercive fields ($H_c > 600\ kA\,m^{-1}$).
[5] Ferro- and ferrimagnetic materials are classified into "hard" (hard to magnetize and demagnetize) and "soft" (easy to magnetize and demagnetize); magnetic materials in between are "semi-hard". The hardness can be measured by the so-called coercivity H_c. When the applied magnetic field H is reduced to zero after saturation, the magnetization M decreases from M_s to the retentivity M_r. The reversed field required to reduce the induction to zero is called coercivity H_c. "Hard" magnetic materials are those with $H_c > 30\ kA\,m^{-1}$ while "soft" magnetic materials are those with $H_c < 1\ kA\,m^{-1}$.
[6] J. M. D. Coey, *J. Magn. Magn. Mater.* **1999**, *196–197*, 1–7.
[7] a) V. I. Matkovich (Ed.), *Boron and Refractory Borides*, Springer, Berlin, **1977**; b) Y. Li, E. Tevaarwerk, R. P. H. Chang, *Chem. Mater.* **2006**, *18*, 2552–2557.
[8] a) E. A. Nagelschmitz, PhD Thesis, University of Cologne, Germany, **1995**; b) R. Feiten, PhD Thesis, RWTH-Aachen, Germany, **1996**.
[9] E. A. Nagelschmitz, W. Jung, *Chem. Mater.* **1998**, *10*, 3189–3195.
[10] E. A. Nagelschmitz, W. Jung, R. Feiten, P. Müller, H. Lueken, *Z. Anorg. Allg. Chem.* **2001**, *627*, 523–532.
[11] R. Dronskowski, K. Korczak, H. Lueken, W. Jung, *Angew. Chem.* **2002**, *114*, 2638–2642; *Angew. Chem. Int. Ed.* **2002**, *41*, 2528–2532.
[12] a) B. P. T. Fokwa, H. Lueken, R. Dronskowski, *Chem. Eur. J.* **2007**, *13*, 6040–6046; b) B. P. T. Fokwa, *Eur. J. Inorg. Chem.* **2010**, 3075–3092; c) VEC of $Sc_2FeRu_5B_2$: 60 = 2×3 (Sc) + 1×8 (Fe) + 5×8 (Ru) + 2×3 (B).
[13] a) G. D. Samolyuk, B. P. T. Fokwa, R. Dronskowski, G. J. Miller, *Phys. Rev. B* **2007**, *76*, 094404_1–12; b) The exchange interactions in series **1** ($Sc_2FeRu_{5-n}Rh_nB_2$) have been studied by first principles density functional calculations (LMTO-type) of the ground state magnetic ordering.
[14] Yu. B. Kuz′ma, Ya. P. Yarmolyuk, *Zh. Strukt. Khim.* **1971**, *12*, 458–461.
[15] J. Brgoch, S. Yeninas, R. Prozorov, G. J. Miller, *J. Solid State Chem.* **2010**, *183*, 2917–2924.
[16] a) B. P. T. Fokwa, M. Hermus, *Inorg. Chem.* **2011**, *50*, 3332–3341; b) M. Hermus, B. P. T. Fokwa, *Z. Anorg. Allg. Chem.* **2011**, DOI: 10.1002/zaac.201100024.
[17] a) B. P. T. Fokwa, R. Dronskowski, *Z. Anorg. Allg. Chem.* **2005**, *631*, 2478–2480; b) B. P. T. Fokwa, B. Eck, R. Dronskowski, *Z. Kristallogr.* **2006**, *221*, 445–449; c) B. P. T. Fokwa, J. von Appen, R. Dronskowski, *Chem. Commun.* **2006**, 4419–4421; d) B. P. T. Fokwa, R. Dronskowski, *J. Alloys Compd.* **2007**, *428*, 84–89; e) B. P. T. Fokwa, G. D. Samolyuk, G. J. Miller, R. Dronskowski, *Inorg. Chem.* **2008**, *47*, 2113–2120; f) B. P. T. Fokwa, *Z. Anorg. Allg. Chem.* **2009**, *635*, 2258–2262.
[18] J. Burghaus, R. Dronskowski, G. J. Miller, *J. Solid State Chem.* **2009**, *182*, 2613–2619.
[19] G. M. Sheldrick, *Acta Crystallogr., Sect. A* **2008**, *64*, 112–122.
[20] S. Hatscher, H. Schilder, H. Lueken, W. Urland, *Pure Appl. Chem.* **2005**, *77*, 497–511.

Received: March 26, 2011
Published Online: June 7, 2011

